

# Development of reactive heat treatments for the synthesis of thin photovoltaic films of Kesterite Cu<sub>2</sub>ZnSnSe<sub>4</sub> through the use of glass boxes

Author: Eduard Alcobé García.

Facultat de Física, Universitat de Barcelona, Diagonal 645, 08028 Barcelona, Spain.\*

Advisors: Alejandro Pérez-Rodríguez and Sergio Giraldo Muñoz

**Abstract:** In the present work, solar photovoltaic cells are formed based on Kesterite. The aim is to synthesize CZTSe absorbers through the use of glass boxes instead of conventional graphite boxes in the reactive heat treatment to improve reproducibility. Various characterization techniques are performed in order to study the morphology, the composition and the crystalline quality of the absorbers, as well as the photovoltaic parameters of the complete solar cell devices.

## I. INTRODUCTION

In recent years, the demand for energy has been continuously increasing [1]. Most energy demand is supplied from the burning of fossil sources such as oil, which are not renewable energies and make an impact on the greenhouse effect, especially due to CO<sub>2</sub> emissions. For this reason, new lines of investigation related to renewable energies such as solar energy have been gaining importance.

Nowadays, there are three different generations of photovoltaic cells. The first is based on silicon, the second on thin film materials (less than 5  $\mu\text{m}$ ) and the third on more advanced concepts approaching the thermodynamic limit.

The work presented in this article was carried out at *Institut de Recerca en Energia de Catalunya (IREC)*. The topic of this work is related to photovoltaic solar energy. Specifically, the solar cells created are based on thin films so they are included in what is called the second generation of solar cells. The solar cells used are made with selenium Kesterite Cu<sub>2</sub>ZnSnSe<sub>4</sub> (CZTSe) which works as an absorber. Kesterite is a quaternary material composed of non-toxic, sustainable and abundant elements which would be included in the second generation as it is used as a thin layer. To synthesize Kesterite, a selenization thermal process is usually required. For this step, a conventional tubular furnace and graphite boxes are typically used.

The aim of this project is to replace graphite boxes with glass boxes (petri dishes) in order to improve reproducibility. Graphite boxes are traditionally used because of their good thermal conductivity. However, graphite absorbs gases formed during the reaction, e.g. SnSe<sub>2</sub>, Se and different impurities from the soda-lime glass substrate such as alkalis. In contrast, glass boxes do not absorb a significant quantity of Se vapor and they can be easily cleaned after every process, although their thermal conductivity is not as good as the graphite's. Therefore, the thermal process might be more difficult to undertake

and may need further optimizations. Nevertheless, reproducibility could be achieved as glass boxes will not be contaminated. Two configurations are evaluated so as to optimize the thermal process. One consists of introducing the glass box into a graphite box although the system is not perfectly hermetically sealed. The other option is simpler as the glass box is placed onto a soda-lime substrate glass (SLG).

## II. PHOTOVOLTAIC TECHNOLOGIES

Typically, a photovoltaic device is what is known as p-n junction. A p-n junction is no more than the union of p-type and n-type semiconductors. As a consequence, a diffusion current appears, as well as the creation of an electric field which leads to a drift current. In equilibrium, a depletion region appears. This zone has a non-zero net charge as there are no mobile carriers but has only fixed ionized impurities (acceptor for the p and donor for the n). Therefore, three distinct regions might be described, the p quasi-neutral zone, the depletion region and the n quasi-neutral zone.

Photovoltaic solar energy is the technology which transforms light directly into electricity by charge carrier separation. Basically, this effect occurs when photons are absorbed by a semiconducting material and the energy of those photons is transferred to the electrons of the semiconductor. Photons need to have more energy than the band-gap in order to be absorbed. Then, an electron has enough energy to jump to a high energetic state leaving behind a hole. The electron promotes from the valence band ( $E_V$ ) to the conduction band ( $E_C$ ). So an electron-hole pair is generated. If this occurs in the depletion region, carriers are separated with a low probability of recombination. Therefore, electrons and holes will be accumulated in n and p regions due to the attraction of donor and acceptor impurities respectively generating a voltage. The movement of these carriers produces a current that can be measured. It is essential to avoid or at least minimize the recombination of these carriers, for this reason a p-n junction to separate them is used [2]. Electron-hole pairs generated at the junction are recollected and the others diffuse to the space charge

---

\*Electronic address: edu.alcobeb@gmail.com

region. Therefore, photons have to be energetic enough to penetrate the top semiconductor (in this investigation, n-type). For this reason, the top semiconductor should be notably thin as their main function is to transmit the solar radiation to the bottom semiconductor.

The complete structure of a thin film solar cell is a group of layers sequentially deposited. From the bottom to the top, a solar cell generally starts with a glass substrate, a molybdenum (Mo) layer, the absorber (p-type semiconductor, Kesterite), the other semiconductor (n-type semiconductor, CdS) to create a heterojunction and finally the window layers of the device (ZnO and ITO) [3]. Also, some intermediate layers can be introduced to alloy or dope the semiconductor. The Mo layer acts as the rear contact and the ITO as the front contact to measure the voltage difference while ZnO has only a protective function.

### III. SAMPLE PREPARATION

First of all, a soda-lime glass substrate is cleaned sequentially with acetone, isopropyl alcohol (IPA) and Milli-Q water in an ultrasonic bath for 10 min for each solvent. Moreover, when changing the SLG from one container to another, the glass is dried with argon.

#### A. Metallic stack precursor deposition

Samples are synthesized by sequential metallic deposition. Samples are prepared on Mo-coated (DC magnetron sputtering, Alliance AC450) soda-lime glass substrates. This Mo layer is in fact divided into three sub-layers with different conductivity and density. The bottom Mo layer is a good conductor with low density to have the best possible bottom contact. The middle layer should be very dense to block diffusion of other elements and prevent undesired selenization. The top layer is a good conductor with low density again, to be sacrificed and form molybdenum diselenide MoSe<sub>2</sub> during the selenization process. The samples are doped with Ge through the evaporation of a 10 nm layer. Then, Cu/Sn/Cu/Zn metals are deposited using DC magnetron sputtering. The composition is calibrated to obtain Zn-rich and Cu-poor samples so as to achieve well-performing devices [4]. After that, an additional 5 nm Ge are evaporated on top of the CZT precursor. Additional details can be found in Ref [5].

#### B. Reactive annealing

The thermal treatment is performed in a tubular furnace under Se atmosphere. Samples are inside a glass box with Se and Sn, 100 mg and 5 mg respectively. These variables are modified in different experiments in order to

optimize the process and determine the best configuration. The conventional annealing process for the synthesis of Kesterite absorbers consists of two steps. The first one is 30 min at 400 °C with a constant Ar flux of 1,5 mbar. Temperature is increased at a rate of 20 °C/min. The second step is 15 min at 550 °C and it is performed at 1 bar, in this case there is no flux. Both time and temperature are variables which can be adjusted to achieve the best possible selenization and to form Kesterite. In this way the CZTSe absorber is synthesized.

#### C. Etching treatments

The surface treatment of these absorber layers is performed by two different etching agents. First 40 seconds dipping time in potassium permanganate (KMnO<sub>4</sub>) is used and is followed by 2 min in ammonium sulfide ((NH<sub>4</sub>)<sub>2</sub>S). The etching processes seek the reduction of surface impurities and secondary phases. KMnO<sub>4</sub> is used to remove ZnSe and (NH<sub>4</sub>)<sub>2</sub>S to etch residual Se from the previous reaction as well as SnSe<sub>2</sub>, while also passivating the surface [6] [7].

#### D. Window layer deposition

A CdS buffer layer (50 nm) is deposited onto the absorber layer by chemical bath deposition (CBD). For this step, a basic medium such as ammonia is needed as well as the use of thiourea. Next, the deposition of the transparent conductive layer (TCO) using DC-pulsed sputtering is performed. This consists of the deposition of ZnO (50 nm) followed by *In<sub>2</sub>O<sub>3</sub> : SnO<sub>2</sub>* (ITO, 200 nm). The ZnO layer's objective is to protect CdS from the sputtering of ITO and cover possible voids that could lead to shunts in the device. Later, lateral isolation is done by means of a microdiamond scribe MR200 OEG to have 3 × 3 mm<sup>2</sup> cells as well as an indium contact to be able to perform the optoelectronic characterization using the solar simulator.

#### E. Glass boxes cleaning

Glass boxes used for annealing may be cleaned after use to ensure next process will not be contaminated. This is a great advantage regarding reproducibility as no selenium, SnSe<sub>2</sub> or other impurities will remain in the box. In contrast, graphite boxes present the problem of Se absorption and it is impossible to remove it. In regard to the required cleaning, a sulfur compound is used. Specifically (NH<sub>4</sub>)<sub>2</sub>S is the one used, although another sulfide such as Na<sub>2</sub>S would have similar effects. Petri dishes are dipped in (NH<sub>4</sub>)<sub>2</sub>S solution for at least 40 minutes and the glass is periodically scrubbed with a cotton stick to ensure cleanliness.

#### IV. CHARACTERIZATION

##### A. X-Ray fluorescence (XRF)

As mentioned previously, the Kesterite absorbers used are not stoichiometric. They are zinc-rich and copper-poor. For this reason, controlling the concentration of elements forming Kesterite is essential. X-Ray fluorescence (XRF) is a non-destructive technique based on exciting the atoms on the sample by bombarding it with high-energy X-rays targeted on a point. The emission of secondary X-rays from the material enables the elemental analysis as well as an estimation of the thickness. The desired ratios between the elemental composition is shown for the CZT and the CZTSe in Table I.

Ratios	d (μm)	$\frac{\text{Cu}}{\text{Zn}+\text{Sn}}$	$\frac{\text{Zn}}{\text{Sn}}$	$\frac{\text{Cu}}{\text{Zn}}$	$\frac{\text{Cu}}{\text{Sn}}$	$\frac{\text{Cu}+\text{Zn}+\text{Sn}}{\text{Se}}$
CZT	0.650	0.72	1.05	1.41	1.48	—
CZTSe	1.600	0.72	1.05	1.41	1.48	<1

TABLE I: Thickness and wanted ratios for the precursor (CZT) and the absorber (CZTSe).

##### B. Solar simulator

A solar simulator is a device which illuminates with a similar spectrum as sunlight. Measuring the photovoltaic current generated by the device as well as the voltage difference, the fill factor and the device efficiency are calculated. The voltage open current ( $V_{OC}$ ) and the current short-circuit ( $I_{SC}$ ) are limiting factors as they are the maximum voltage and current respectively from a solar cell. The fill factor (FF) is the ratio of the maximum power from the solar cell to the product of  $V_{OC}$  and  $I_{SC}$ . While the efficiency ( $\eta$ ) is the ratio of energy output from the solar cell to input energy from the sun.

$$\eta = \frac{V_{OC}I_{SC}FF}{P_{in}}.$$

Two measures with the solar simulator are done, one before heating with a hot plate and one after. The hot plate consist in heating samples at 250°C during 25 minutes in air, and it has been shown to be effective to improve devices' performance [8].

##### C. Scanning Electron Microscope (SEM)

A scanning electron microscope is an electron microscope which produces images of a sample by scanning the surface using a focused electron beam. Primary electrons emitted by the source are accelerated and focused on a target with an energy of 5 keV. The working distance (distance between gun and sample) is approximately 5 mm. Emitted electrons and the sample have an inelastic interaction and secondary electrons (SE) are generated.

Only the most superficial SE reach the detector as they have enough energy to escape from the sample. Therefore, SEM technique enables the study of the morphology of the sample as it is a superficial technique (around 10 nm of penetration depending on the applied voltage).

##### D. Raman spectroscopy

Raman spectroscopy is a superficial characterization technique used to study structural properties and to identify chemical phases. It uses a laser (a 532 nm green laser was used) which excites vibration modes of atoms and molecules through inelastic interaction between incident photons and the sample. Those modes are identified as peaks of intensity in the spectra detected thanks to the scattered infrared light (Raman shift).

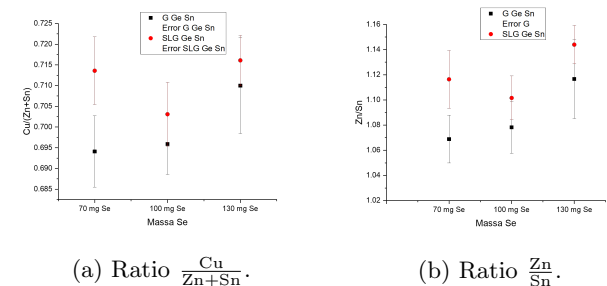
$$\delta\tilde{\nu} = \left( \frac{1}{\lambda_0} - \frac{1}{\lambda_1} \right).$$

Where  $\lambda_0$  is the excitation wavelength and  $\lambda_1$  is the Raman scatter wavelength. The position of the peak, or in other words the shift in energy, is informative of the vibrational modes. Additionally, the area of a peak notify about how crystalline the sample is, as it is related with the number of phonons describing the crystal structure.

#### V. ANALYSIS AND RESULTS

During this investigation, different samples were fabricated in order to study the effect of a number of parameters. The variables of interest are the presence of Sn and the mass of Se inside the petri dish as well as the annealing temperature and time.

The effect of the mass of Se on the sample's composition is shown in Fig.(1). The amount of Cu versus Zn+Sn is closer to the optimum, for the SLG configuration than the glass box inside the graphite box (Fig.(1a)) although it presents less Sn related with Zn (Fig.(1b)) and more related with Cu (Fig.(1d)). Fig.(1c) shows that the ratio of Cu to Zn is no different between configurations and nor is Se mass. Then, it is assumed that Sn is the most difficult element to control. Moreover, a systematic excess of Zn compared to the desired ratios in Table I is appreciated. Selenization is adequate in all samples (Fig.(1e)).



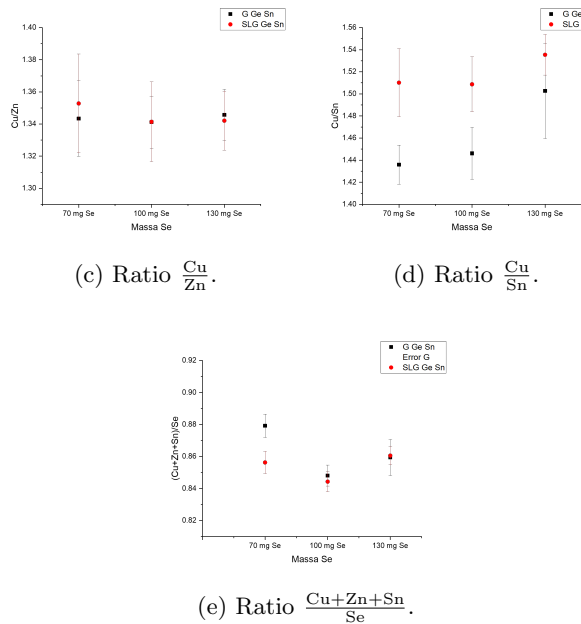


FIG. 1: Different ratios for samples with the glass box inside a graphite box (G Ge Sn) and with the petri dish onto SLG (SLG Ge Sn) with Se mass variations.

The SEM images of the samples in glass boxes are compared with an image of a “conventional” Kesterite synthesized in a graphite box (Fig.(2a)). No differences are appreciated between the two used glass boxes configurations. However, interesting results are found in relation to the presence or not of Sn powder during the annealing. Fig.(2b) and Fig.(2c) are respectively images of samples with and without Sn. Interestingly, samples with Sn have significantly better morphology, showing larger grains with a more compact structure than samples without Sn, possibly meaning that Sn helps the synthesis. However, comparing the Sn-containing sample to the reference sample, it looks slightly rougher and not perfectly crystallized yet.

Raman results are shown in Fig.(3a) and Fig.(3b) comparing the reference sample with two samples with the configuration of petri dish inside a graphite box and the two others with the glass box directly onto SLG. For both configuration there is a sample with Sn and another without Sn. As clearly seen, all the Raman spectra shows the main characteristic peaks of the Kesterite CZTSe phase located at about  $174\text{ cm}^{-1}$  and  $196\text{ cm}^{-1}$ , and the series of peaks between  $220\text{--}260\text{ cm}^{-1}$ . From these spectra, no additional secondary phases are detected in any of the samples in their surface. However, the penetration is  $\sim 150\text{ nm}$ , therefore it can not be discarded the presence of other phases deeper in the bulk. The most remarkable difference among the samples is the intensity of the peak at  $174\text{ cm}^{-1}$ , which is usually related to the Cu concentration (or Cu vacancies). Nonetheless, it remains difficult to interpret having only a small set of samples, and could also be related to some inhomogeneities.

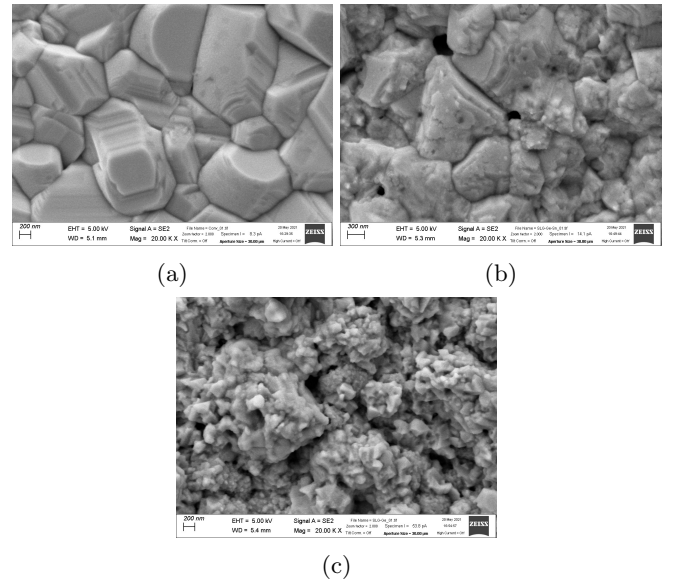


FIG. 2: SEM images. (a) is from the reference sample obtained using a graphite box, (b) is from a sample with Sn obtained using a glass box and (c) from a sample without Sn obtained using a glass box.

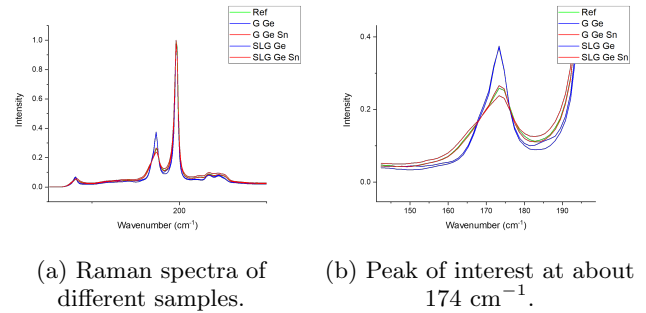


FIG. 3: Raman spectra

The most important parameter for a solar cell is the efficiency as the final objective is to convert the maximum amount of solar light to electrical current. Table II shows the efficiencies achieved in some of the samples in order to compare both configuration with glass box (the one with graphite box and the other one with SLG) as well as the impact of Sn and annealing’s temperature. The reference sample has a surprisingly low efficiency. The most probable reason is the failure in some of the steps and specifically the most reasonable hypothesis is that the evaporation did not work correctly and some cross-contamination might have occurred from the evaporation of other elements such as Fe (possibly from the clamps). As it is well-known in the Kesterite community, even very small quantities of Fe can be very detrimental for the devices, by introducing harmful defects in the material.

Nevertheless, as all samples compared are from the same batch of precursor, data could be taken into consideration to some extent. Therefore, the fact that the

reference has poorer efficiency than the samples annealed with glass box could be a satisfactory indicator. In addition, the samples with SLG has systematically better efficiency than the ones with graphite. Moreover, the presence of Sn in powder during the annealing is beneficial as higher efficiencies are accomplished. This correlates notably well with the better morphology observed by SEM for the samples synthesized with additional Sn during the selenization process (Fig.(2)). Furthermore, increasing the temperature during the second step of the annealing appears to be beneficial. Another interesting factor is the effect of the hotplate post-annealing which seems harmful for the samples without extra Sn while it helps in the samples with Sn. The optimization of the hotplate might be another point to focus on in the future.

Configuration	Before hotplate	After hotplate
Reference	0.26 (0.59)	0.38 (0.73)
G Ge	0.68 (1.11)	0.44 (0.68)
SLG Ge	1.15 (1.29)	0.51 (0.62)
G Ge Sn	0.54 (0.85)	1.09 (1.55)
SLG Ge Sn	0.92 (1.16)	1.60 (2.16)
SLG Ge Sn 565°C	1.67 (1.93)	1.75 (2.20)
SLG Ge Sn 580°C	1.15 (1.45)	1.39 (1.74)

TABLE II: Mean efficiency  $\eta$  (maximum efficiency) of studied samples, the reference is Kestertite synthesized with graphite box. G indicates petri dish inside a graphite box and SLG that the glass box is onto SLG.

## VI. CONCLUSION

- The mass of Se does not have a remarkable impact on the composition of samples as long as a minimum amount of Se is available to synthesize Kesterite (Se saturated atmosphere).
- According to the SEM images as well as the efficiency values, the presence of Sn powder seems

essential to perform the selenization reaction. It helps the nucleation of Kesterite grains and acts as a catalyst of the reaction. Furthermore, the formation of  $\text{SnSe}_2$  in the reactive atmosphere minimize the creation of this secondary phase in the sample.

- From the Raman characterization, no relevant undesired secondary phases are detected at the surface (first 150 nm) in any of the studied samples. Moreover, the crystalline quality seems comparable for all of them at surface level, although a deeper analysis with more sample would be necessary to confirm the observations.
- No notable difference are appreciated between both configurations. Nevertheless if the aim is not to use graphite boxes, then the configuration with just a SLG to hold the petri dish should be taken in to superior consideration. Moreover the efficiencies are systematically higher although there is not an extremely significant variation.
- The annealing temperature and time are sensitive parameters to optimize the formation of Kesterite. A slightly increment of temperature seems to help the nucleation of Kesterite as higher efficiencies are measured with the SLG configuration. However, more experiments should be carried out in order to optimize the temperature.

## Acknowledgments

I would like to sincerely thank my advisors Alejandro Pérez-Rodríguez and Sergio Giraldo Muñoz for their guidance in my work and the opportunity to work in a real investigation laboratory such IREC. Also, I want to thank Alex Jiménez Arguijo to teach me, solve my doubts and follow my work. Finally, I want to thank my family and my friends for their support.

- 
- [1] World energy demand growth rate, 2011-2019. IEA, Paris.  
[2] PV Education. 2021. Solar Cell Operation. <https://www.pveducation.org/pvcdrom/solar-cell-operation/light-generated-current>.  
[3] PV Education. 2021. Solar Cell Structure. <https://www.pveducation.org/pvcdrom/solar-cell-operation/solar-cell-structure>.  
[4] Choubrac, L., et al. 2012. Structure Flexibility of the  $\text{Cu}_2\text{ZnSnS}_4$  Absorber in Low-Cost Photovoltaic Cells: From the Stoichiometric to the Copper-Poor Compounds. Inorganic Chemistry. DOI:10.1021/ic202569q.  
[5] Giraldo, S., et al. 2018. How small amounts of Ge modify the formation pathways and crystallization of kesterites. Energy & Environmental Science; 11(3), pp.582-593. DOI:10.1039/C7EE02318A.  
[6] Xie H, et.al. 2014. Impact of Sn(S,Se) secondary phases in  $\text{Cu}_2\text{ZnSn}(S,\text{Se})_4$  solar cells: a chemical route for their selective removal and absorber surface passivation. ACS Applied Materials and Interfaces; 25: 2–6. DOI:10.1021/am502609c.  
[7] López-Marino S, et.al. 2013 ZnSe etching of Zn-rich  $\text{Cu}_2\text{ZnSnSe}_4$ : an oxidation route for improved solar-cell efficiency. Chemistry - A European Journal; 19: 14814–14822. DOI:10.1002/chem.201302589.  
[8] Dimitrievska, M, et al. 2016. Raman scattering analysis of the surface chemistry of kesterites: Impact of post-deposition annealing and Cu/Zn reordering on solar cell performance. Solar Energy Materials and Solar Cells; 157, pp.462-467. DOI:10.1016/j.solmat.2016.07.009.